Stratigraphical reassessment of Grotta Romanelli sheds light on Middle-Late Pleistocene palaeoenvironments, sea-level history and human settling in the Mediterranean

Pierluigi Pieruccini
Università di Torino
Luca Forti (luca.forti@unimi.it)
Università degli Studi di Milano
Beniamino Mecozzi
"Sapienza" Università di Roma
Alessio Iannucci
"Sapienza" Università di Roma
Tsai-Luen Yu
National Academy of Marine Research
Chuan-Chou Shen
National Taiwan University
Fabio Bona
Università degli Studi di Milano
Giuseppe Lembo
Ministero dell'Istruzione
Brunella Muttillo
Università di Ferrara
Raffaele Sardella
"Sapienza" Università di Roma
Ilaria Mazzini
Consiglio Nazionale delle Ricerche (CNR)

Article

Keywords:

Posted Date: April 18th, 2022

DOI: https://doi.org/10.21203/rs.3.rs-1527156/v1

Abstract

During the last century, Grotta Romanelli (Southern Italy) has been a reference site for the European Late Pleistocene stratigraphy, due to its geomorphological setting and archaeological and palaeontological content. The beginning of the sedimentation inside the cave was attributed to MISs 5e and the oldest unearthed evidence of human occupation, including remains of hearths, was therefore referred to the Middle Palaeolithic. Recent surveys and excavations produced new U/Th dates, palaeoenvironmental interpretation and a litho-, morpho- and chrono-stratigraphical reassessment, placing the oldest human frequentation of the cave between MIS 9 and MIS 7, therefore embracing Glacial and Interglacial cycles. These new data provide evidence that the sea reached the cave during the Middle Pleistocene and human occupation occurred long before MISs 5e and persisted beyond the Pleistocene- Holocene boundary.

Introduction

The Italian territory is rich in stratigraphic records from caves and rock shelters bearing archaeological findings that have contributed to the framework of the Quaternary stratigraphy in Europe. Recent research on iconic Italian sites revealed the importance of their chrono-, litho-, morpho- and bio-stratigraphical reassessment, considering the progresses that stratigraphy, palaeontology, and archaeology have made in the last 100 years (1, 2, 3, 4, 5). In particular the Apulian region (Southern Italy) (Fig. 1a), several caves and rock shelters formed in a typical Mediterranean karst landscape (8) preserved important records of long-term environmental change and prehistoric human activity (6, 7, 8). Many of these caves are facing the seashore nowadays. Their litho- and morpho-stratigraphical records provide information about Quaternary sea-level history (9, 10, 11, 12, 13), palaeoenvironments (16) and their relationships with human settlements. These caves also record direct evidence of Homo neanderthalensis King, 1864 (i.e., Grotta di Lamalunga, 14) and the earliest European occurrence of Homo sapiens Linnaeus, 1758 (i.e., Grotta del Cavallo, 15) (Fig. 1b).

Grotta Romanelli opens into Cretaceous limestone along the cliffs of the southeastern coast of Apulia (Fig. 1c). Since the beginning of the 20th century, Blanc and others systematically excavated and described the infilling deposits of the cave and its content (reference therein in 17, 18) (Suppl. Mat. 1, Fig. S1 in Suppl. Mat). The cave soon became a reference for Quaternary geomorphological and geological studies for the assessment of the Last Interglacial Sea level in this area of the Mediterranean (19, 9). The deposits infilling the cave and the palaeo sea-level (PSL) indicators, such as marine notches, Lithophaga burrows and algal encrustation markers of relative sea-level (RSL), were referred to the MISs 5e marine highstand (20, 21). Within the cave, the PSL indicators are well preserved as they were buried by a succession made of, from bottom to top, sandy pebbles beach deposits, angular breccia and the sequence of the so-called “Terre Rosse” and “Terre Brune”, silty-sands deposits originally considered of aeolian origin (20, 21). The chrono-stratigraphical framework proposed by the first researchers was supported by two U/Th dates on stalagmitic layers and nine radiocarbon dates on charcoal and humic acids (22, 23, 24). Following the correlation to MISs 5e for the beginning of the sedimentation inside the cave, the impressive fossil record of birds and mammals, together with portable art and parietal

engravings, hearts, and limestone or flinty lithic tools was referred to the time span MIS 5 – 1, also documenting the Last Glacial Maximum with the finding of the iconic Great Auk Pinguinus impennis (Linnaeus, 1758) (= Alca impennis) (20, 25). The archaeological and palaeontological findings from Grotta Romanelli, hosted in museums and institutions across Italy, have been the subject of several studies, both confirming (26, 27) or questioning (28, 29, 30) the chrono-stratigraphic setting proposed by Blanc (20). Recently, new excavations led to a reassessment of the stratigraphy of the uppermost part of the cave infilling (31) and a partial revision of some of the palaeontological remains (32, 33, 34, 35). Furthermore, a critical review of the Last Interglacial PSLs' along the stable coasts of the Mediterranean Sea (11), indicated the highest Grotta Romanelli's notch as older than MISs 5e. Here we present new U/Th ages, coupled with new litho- and morpho-stratigraphical evidence from the 6 m thick sequence still preserved inside the cave and the sedimentary record and geomorphological features found along the cliff in its immediate surroundings, revising the age of the lowermost cave infilling and the palaeoenvironmental interpretation proposed by Blanc (20, 21). Moreover, for the first time, we present evidence of litho- and morpho-stratigraphical units on the cliff above e below the cave entrance, which, bounded to the chrono-stratigraphical data of the cave deposits, provide new information for the Middle Pleistocene sea-level history of this area of the Mediterranean.

Results

During the new excavations four sections were opened inside the cave for stratigraphical and sedimentological observations coupled with geochronological (U/Th) and micromorphological sampling (Table 1, Suppl. Mat. 2, Fig. S2, S3 and Table S1 in Suppl. Mat.). Moreover, new geomorphological and geological surveys outside the cave were carried out. The litho- and morpho-stratigraphical settings of the succession inside the cave and those observed out of the cave are herein described, providing information on the corresponding sedimentary environments and their palaeoenvironmental significance.

Cave litho-, morpho-stratigraphy and related sedimentary environments

Today, the infilling sedimentary succession is cropping out only in the innermost part of the cave due to the impressive volume of sediments excavated by Blanc and afterwards (Fig. 2a, Suppl.Mat.1). Originally completely filling the cave, the succession shows differences in thickness, geometry, and sedimentary facies according to the sectors of the cave where the sections are opened and the morphology of the bedrock (Fig. 2b). The basal part of the sediments fills solution and erosional features formed earlier on the floor and on the sides, both in vadose and subaerial conditions when the cave was already open to marine ingression. These features, undercutting the bedrock, consist of : i) a basal erosional scour that enters the cave for about 25 m from the entrance, large max 2 m and getting narrower toward the inner part and ii) two marine notches (mn), more evident on the northern side of the cave. The higher notch (mn1) is found at 9,2 m a.s.l. and the lower notch (mn2) at 7 m a.s.l. Both notches are characterised by the presence of algal encrustation and abundant Lithophaga burrows (Fig. 2c). The lithostratigraphical setting can be broadly subdivided into two parts: coarse- to very coarse-grained limestone gravels, pebbles, and boulders in the lowermost part of the succession; abruptly changing upwards to fine-grained

silts, clays and sands containing lenses of angular to subangular fine- to coarse-grained limestone gravels. A wedge-shaped roof spall is interbedded within the finer grained part of the succession. The main bounding surfaces are mostly horizontal or undulated. On the four sections opened inside the cave during the 2017-2021 campaigns, referred to as North (N), South (S), North-West (NW) and West (W) (Table 1, Fig. 2), five stratigraphic units were recognised (Table 1, Fig. 3). Moreover, six stratigraphic units were identified outside the cave along the cliff at higher or lower elevation or partially covering the cave entrance. Stratigraphic units are named with the prefix I or O indicating their identification Inside or Outside the cave, respectively (Table 1).

Overall view of the cave from the northern side with the location of the described sections (b). The two marine notches (mn1 and mn2) carved into the bedrock and observable on the northern side of the cave, originally buried by the sedimentary succession (c). Artwork and photo PP, LF.

Table 1: Sedimentary characteristics of the stratigraphic units (SU). Prefix I for SUs' inside the cave, prefix O for SUs' outside the cave. The abbreviations of archaeological and palaeontological findings refer to the new excavation, except when in bold (literature record). Legend: A – Aves; Am – Amphibia; Bt – Bone tools; C – Crustacea; E – Echinodermata; Ft – Flint tools; For – Foraminifera; H – Hearts; Hr – Human remains; Lt – Limestone tools; M - Mammal; mMal – marine Malacofauna; cMal - continental Malacofauna; Ost – Ostracods; P – Pisces; Pa – Portable Art; R – Reptilia. (References 37,20,21,38, 28,39,40,34,35)

Stratigraphic Units this work	Main sedimentary characteristics	Stratigraphic Units Blanc (1920)	Archaeological findings	Fossil findings
INSIDE THE CAVE				
ISU5	Thinly to medium layered sands, silts and clays with stone lines and lenses of matrix-supported angular to subangular fine to coarse-grained monogenic limestone gravels	**A,B,C,D,E**	**Bt, Ft, H, Pa**	**A,** Am, E, **Hr, M,** cMal, mMal, **P,** R
ISU4	Roofspall made of open-work angular to subangular monogenic limestone boulders, cobbles and gravels, whose voids are infilled by sediments coming from the overlying ISU5. The top of ISU4 is locally draped by a flowstone up to 8 cm thick.	**F**		
ISU3	Clays and silts with variable amounts of fine to coarse-grained quartz sands and rare scattered fine to coarse angular to subangular monogenic limestone strongly weathered gravels. In Section S, W and NW the top of this unit is locally draped by a discontinuous flowstone (Level F of Blanc, 1920) from a few mm to several cm thick. In section NW irregular impregnative carbonate crusts are also present.	**G**	**Lt**	**A,** Am, E, **M,** cMal, **P,** R
ISU2	Wavy bedded unsorted angular to subangular open-work to matrix supported coarse-to very-coarse grained limestone gravels, pebbles and boulders, with dark brown to yellowish brown sandy-silty matrix. Very rare rounded to sub rounded pebbles. The	**H** **I**	**H, Ft, Lt**	**A, Am,** C, E, M, cMal, **mMal,** P

	top of this unit is locally characterised by the presence of an irregular flowstone (Level H of Blanc,1920) whereas other flowstones and impregnative carbonate crusts locally also cap the lower beds.			
ISU1	Rounded to subrounded polygenic limestone gravels, pebbles and boulders with variable amounts of sandy-silty matrix, resting over the bedrock. Locally, it contains rounded to subrounded re-worked pumices. Occurrence of foraminifera, ostracoda and molluscs.	**K**	H, **Lt**	For, **mMal,** Ost
OUTSIDE THE CAVE				
OSU6	Thinly bedded breccia dipping seaward up to 30° made of fine- to coarse-grained, angular to subangular, strongly cemented limestone flake-shaped gravels, open-work to matrix supported.			
OSU5	Roughly bedded breccia dipping seaward up to 40° made of unsorted, coarse- to very coarse-grained, strongly cemented, mostly open-work limestone boulders, pebbles and gravels, unconformably overlying OSU4 and OSU3			
OSU4	Roughly horizontally bedded or slightly seaward dipping, unsorted angular to subangular, strongly cemented limestone gravels, cobbles and boulders, from open work to matrix supported. Rounded to sub rounded pebbles and gravels are found in the lowermost beds that bury unconformably the			M

	underlying OSU3. Some of the boulders are made of OSU2.		
OSU3	Roughly bedded and strongly cemented conglomerates made of unsorted, subrounded to rounded and subangular polygenic limestone gravels, cobbles and boulders resting over an almost flat abrasion platform carved on the bedrock between ca. 3,8 m a.s.l. and 4,8 m a.s.l.		
OSU2	Gently dipping bedded and cemented breccia made of unsorted coarse to very coarse, monogenic, angular to subangular limestone gravels, pebbles and boulders, from open work to matrix supported.		M
OSU1	Packed to cemented bedded conglomerates made of massive, unsorted, polygenic, coarse-to very coarse rounded to subrounded, unsorted polygenic limestone gravels, pebbles and cobbles. They bury a flat or slightly undulated basal surface carved on the bedrock and to the south is unconformably overlaid by OSU2.		

Out of Cave Morpho- and Litho- stratigraphy

Outside the cave, both in the upper and the lower part of the cliff, further evidence of morpho- and lithostratigraphic units have been observed and described (Table 1, Fig. 4). They represent two phases, depositional and erosional, related to marine high stands older and younger than those observed within the cave. In both cases, high-stand marine deposits are buried under low-stand debris-slope deposits. On the cliff next to the cave entrance, three marine notches are preserved, namely mn1 at 9 m, mn2 at 7 m and mn3 at 5.5 m a.s.l (Fig.4a, Fig.4e). In detail, mn1 and mn2 are the out-of-cave continuations of the notches observed within the cave, where they have a lateral continuity of about 15 m (Fig. 4a.1). At the

cave entrance, the two notches (mn1 and mn2) are continuous, the higher is wider and deeper (1.4 m and 0.7 m) than the lower (1 m and 0.4 m) and their morphology suggests their formation during rising RSL (41, 42, 43). They are also characterised by a continuous riddling by Lithophaga holes, whereas only mn1 preserves a vermetid reef. Mn3 is found only below the cave entrance, it is laterally preserved for about 1.5 m, its width is 1.1 m, and it is partially covered by small patches of cemented reddish matrix gravels whereas to the south it is almost completely buried by the OSU3 gravels (Fig. 4a.2, Fig. 4d). Above Grotta Romanelli, a terrace at about 18 m a.s.l. is still preserved and carved on an ossiferous cemented breccia made of coarse unsorted gravel from open work to matrix supported (OSU2) (Fig. 4b). In the northern sector of the bay, a conglomerate made of unsorted polygenic pebbles and cobbles (OSU1) bury a surface carved on the bedrock that is unconformably overlain by OSU2 to the south (Fig. 4c).

Discussion

Grotta Romanelli and its chronological and palaeoenvironmental framework.

New fieldwork at Grotta Romanelli allowed a litho-, morpho- and chronostratigraphical assessment of the successions inside and outside the cave. This achievement is of paramount importance since the former chronostratigraphical setting of Grotta Romanelli, placed the beginning of the sedimentation inside the cave during MISs 5e and became a paradigm for Quaternary archaeology, palaeoanthropology, palaeontology, stratigraphy and sea-level history of Italy and the Mediterranean (20). In Grotta Romanelli, the sedimentary evidence points to the deposition within an active humid karst setting (6). Moreover, the position of the cave relative to the sea increases its importance concerning the geodynamics and the eustatic history of this sector of the Mediterranean (44). In fact, the position of the water table in the coastal zone is linked to eustatic sea-level changes (45) and the succession within Grotta Romanelli is one of the older in-cave marine sedimentary records not ‘blown-out’ by high rates of water flow. After the works of Blanc (20, 21) (Suppl.Mat.1) the PSL indicators within the cave (mn1 and mn2 in Fig. 2 and Fig. 3) were considered coeval with and associated to the coarse-grained basal part of the sequence, which included both ISU1 and ISU2, and were attributed to the Last Interglacial. This morpho-stratigraphical assumption was based on the observation that these were the only PSL higher than the present-day sea level along the cliff of Grotta Romanelli. Our research brought new evidence based on litho-stratigraphical, morpho-stratigraphical and geochronological data depicting a different history of Grotta Romanelli during the Quaternary. ISU1 is the only sedimentary RSL marker within Grotta Romanelli, deposited in a coastal marine environment where the finer-grained sediments were preserved only in small conservative features, such as potholes carved within the bedrock, whereas gravels, pebbles and cobbles entered the cave during high-energy events. Moreover, it is found as a lag resting over mn2, the lower marine notch carved on the bedrock. Outside of the cave, above and below the cave entrance, two others sedimentary RSL markers and one PSL (mn3) are for the first time found and described: OSU1 located at ca. 18 m a.s.l. (Fig. 4c), OSU3 found at ca. 3.8 m a.s.l. (Fig. 4d, Fig. 4e) and mn3 at 5.5 m a.s.l (Fig. 4a.2). Therefore, RSL and PSL markers, sediments and marine notches found within Grotta Romanelli cannot be uniquely associated with the Last Interglacial. ISU2 provides the older geochronological constraint for the whole succession. In fact, two U/Th dates, made on the flowstones

embedded within ISU2 in the N sector (Fig. 5), provided ages of 360 ± 87 ka and 218.8 ± 34 ka (Table S1 in Suppl.Mat.) respectively from the lower-mid part and the top of the Unit. Furthermore, the flowstone formed on top of the bedrock is dated to 325 ± 39 ka in sect. N buried under ISU2 (Fig. 5). This chronology indicates that the marine deposition of ISU1 should be dated back to the Middle Pleistocene. ISU2 is made of autochthonous debris derived from the ceiling and walls of the cave or from short-distance mass-deposition, re-worked within the cave according to the floor morphology. Partial transport by water run-off is also suggested by the rough trough crossbedding and by the rare presence of re-worked rounded marine pebbles, cannibalised from the underlying ISU1. Periods of non-deposition are indicated by the precipitation of carbonates forming the wavy irregular flowstone on top of the beds (Fig. 3) and by the local presence at the bottom of phytoclastic beds, possibly related to local small ponds with standing carbonate-rich water. The origin of the coarse-grained angular debris of ISU2 is associated with rock degradation and stress release from the cave ceilings and walls, lacking any other palaeoenvironmental markers such as freeze-thaw features or frost slabs. Therefore, the presence and distribution of sediments belonging to ISU2 does not provide specific palaeoclimatic nor palaeoenvironmental indications being mainly associated with the morphology of the cave (6, 46). The deposition of ISU2, according to the U/Th dates, occurred across a long timespan, suggesting that during this part of the Middle Pleistocene the cave was almost empty and that it underwent scarce, mainly autochthonous depositional events, also incorporating the older evidence of human and animals' frequentation of the cave, including fire features, limestone lithic tools and burnt and unburnt bones (20, 21).

Depositional environment and dynamics suddenly changed after ISU2, which is paraconformably buried by ISU3, macroscopically characterised by reddish colour ("Terre Rosse"). ISU3 is made of thinly layered planarly or cross-bedded silts, clays and sands indicating aqueous deposition through low-energy runoff. The lack of any evidence of in situ clay illuviation or other long-term soil-formation related features suggests that the iron-enrichment and the carbonate leaching of the groundmass is derived from the erosion of leached, argillic limestone soils in the overlying plateau and surrounding slopes. In fact, the sandy and silty mineral fraction of ISU3 is made primarily of quartz suggesting its provenance from the erosion of aeolian deposits such as coastal dunes or other older deposits originally present on top of the plateaux (i.e. OSU1) or from colluvial sediments or soils covering the surrounding landscape. The sediments therefore have been washed into the cave system and transported by run-off and/or karstic waters, indicating the beginning of landscape destabilisation (47) within a warm and humid climatic context as suggested also by the presence of pollen spectra with a consistent amount of olive tree (48). Once arrived inside the cave the sediments were redistributed over short distances by bi-directional water flows both toward the internal and the external part of the cave, by means of predominant sheet-flows (plane parallel bedding) and occasionally within small channels (local cut and fill), possibly related to events of increased water availability (i.e. strong rainfall) alternating with periods of standing water (fining-upward trends and laminated clays) (Fig. S3d in Suppl.Mat.). Contemporaneous physical weathering of the bedrock within the cave provided the coarse-grained autochthonous carbonate fragments. Although the lack of evidence of dense vegetation, phases of non-deposition are highlighted by the common presence of biological voids, including chambers and channels (Fig.S3c in Suppl.Mat.),

burrowing features, faecal pellets and locally small-sized coprolites. Rare elements of anthropogenic origin (i.e. burnt bone fragments) and fire-related origin (charcoals and charred plant tissues) (Fig. S3a, Fig. 3b in Suppl.Mat) also suggest a short-distance transport of anthropogenic deposits within the cave system. In the N and S sector of the cave, ISU3 is buried under a roof spall (ISU4 in Fig. 3) covered by a flowstone dated at 112.5 ± 1 ka (N sector, Fig. 5, Table S1 in Suppl.Mat.) and 74 ± 6 ka (S sector, Fig. 5, Table S1 in Suppl.Mat). Assuming that the age of the speleothem might reflect a long period of non-deposition within the cave and dipping vadose waters with precipitation of calcite, these ages post-date the deposition of ISU3 at least at the beginning of the Late Pleistocene. Due to the “colluvial” nature of the sediments inherited by the erosion of Interglacial leached soils ISU3 can be correlated to the early phases of climate deterioration that followed the Last Interglacial (i.e., MISs 5d-b). ISU3 and ISU4 are in turn buried by ISU5, the so-called “Terre Brune " (due to their brownish colours) of Blanc (20) (Fig. 5). The sedimentary characteristics are very similar to those of ISU3 and point to deposition in a low-energy sheet-wash and runoff environment alternating with phases of standing water within local ponds formed by consecutive events (Fig. S3e, Fig.S3f in Suppl.Mat.), although the lack of major discontinuities within the succession suggests that it was probably laid down at a regular pace. The random distribution of cross bedding dip suggests a direction of sediments transport according to local irregular morphology, i.e. the top of ISU4 that dammed the inner part of the cave, where finer grained sedimentation prevailed, and concentrated the coarser grained deposition in the southernmost sector of the cave (Sect. S in Fig. 3) where a broad and shallow channel was filled by coarser-grained sediments including bedrock boulders and cobbles. Similarly, to ISU3, there is no evidence of soil formation features and the composition suggests the re-working of both ISU4 (limestone gravelly fraction) and ISU3 (colluviated reddish clays, Fig.S3g in Suppl.Mat). The overall brownish colour and the lack of iron sesquioxide’s precipitation, together with the abundance of plant tissues, also suggests a sediments’ source from the erosion of brown soils covering the slopes surrounding the cave washed within the cave. Moreover, the abundance of anthropogenic components, such as charcoal fragments, bones (Fig.S3h in Suppl.Mat) locally with evidence of thermal impact, charcoals and charred plant remains, indicate the reworking of anthropic deposits from other sectors of the cave (35). However, most of the anthropogenic components are reduced in size and with seldom evidence of weathering or secondary impregnation by phosphate (Fig. S3g in Suppl. Mat) and their origin should be related to short-distance re-working within the cave, lacking any features that could be linked to trampling or crushing. ISU5 almost completely filled the cave up to the roof and its chronology can be constrained by the age of the speleothem found on top of ISU3 in the W sector, which provided a U/Th age of 43.3 ± 8 ka (Fig. 5, Table S1 in Suppl. Mat.). Moreover, radiocarbon dates of the same Unit in the S, W and SW sectors of the cave, provided ages for its deposition between 13,6 cal ka BP and 11,4 cal ka BP (31, 49) indicating high sedimentation rates at the Pleistocene-Holocene transition. Such rapid sedimentation occurred by both erosion of the surrounding landscape and related sediments and soil covers and partial re-working of the older succession within the cave, including the autochthonous coarse-grained gravels and cobbles of bedrock produced by the degradation of the cave walls and ceiling.

The reconstruction of sea-level history and palaeo-climatic implications.

Relative sea level (RSL) markers at Grotta Romanelli are of two types: deposits and PSL indicators, mainly marine notches. PSL are found within the cave, from the higher to the lower, namely mn1 at 9.2 m a.s.l., mn2 at 7 m a.s.l., ISU1, as well as the RSL marker represented by ISU1 (Fig. 3, Fig. 4). A PSL marker is also located along the cliff, below the cave entrance (mn3 at 5.5 m a.s.l. in Fig. 4a,Fig. 4d, Fig. 4e). On the same cliff, above and below the cave entrance two RSL markers are respectively located at 18 m (OSU1 in Fig. 4c), and between 3.8 m and 4.8 m a.s.l. (OSU3 in Fig. 4a,Fig. 4d, Fig. 4e). The highest RSL marker (Fig. 4c), OSU1, indicates a high-energy littoral deposition over a marine abrasion platform modelled during a marine highstand. The intermediate RSL, ISU1, found inside the cave is associated with the tidal notches mn1 (9 m a.s.l.) and mn2 (7 m a.s.l.) with Lithophaga burrows. Assuming mn1 and mn2 as belonging to the same transgressive phase (43) and dated before 320 ka BP (the average lower age of the overlaying ISU2) should be associated to the highstand of the MIS 9 (Fig. 6, Fig. 7), as already debated by Mastronuzzi et al., (9) and Antonioli et al., (11) based on correlation with the elevation of other marine notches along the tectonically stable Apulian and Italian coasts. This attribution dismantles the Grotta Romanelli paradigm (20) of the Last Interglacial age for the marine features and deposits found within the cave. A further consequence of this chronological setting is the possible attribution of the older marine record represented by OSU1 to the highstand of the MIS 11 (Fig. 6, Fig. 7), although currently, a standardised review of pre-MIS 5 Mediterranean sea-level proxies is not available (50). This Middle Pleistocene marine high-stand deposit was followed by an erosional regressional phase (MIS 10) marked by typical low-stand and cooler climate indicator debris-slope unit (OSU2) (Fig. 4a, Fig. 4b). Moreover, the finding of the marine terrace located just below the entrance of Grotta Romanelli (Fig. 4d) brings new light to the Last Interglacial sea-level of this sector of the Mediterranean. In fact, the inner tip of the top of the deposit characteristic of high-energy littoral environment reaches 4.8 m a.s.l. and rests over a marine abrasion platform carved over the bedrock at an elevation of ca. 3.8 m a.s.l. The terrace is linked to the mn3 located at 5.5 m a.s.l. in front of the cave entrance (Fig. 4, Fig. 6, Fig. 7) that can be correlated to the MISs 5e, with an elevation within the variability for the same highstand in the same area of the Mediterranean (9, 11, 50). After the Last Interglacial, the sea level lowstand and climate deterioration were followed by the emplacement of the thick debris units (OSU4, 5 and 6 in Fig. 4, Fig. 6, Fig. 7) that partially buried the cave entrance and were dismantled during the history of the excavations. OSU4 accumulated on top of OSU3, the MISs 5e terrace, and the chaotic setting as well as the presence of boulders made of cemented stratified breccias and the occasional presence of rounded pebbles indicates that it originated by rockfalls originated by OSU1 and OSU2 from the overhanging cliff (Fig. 4). The subsequent OSU5 shows a thick layer dipping up to 35 degrees according to the slope, burying both OSU3 and OSU4 and dip below the present-day sea level (Fig. 4), marking its deposition during a well-established lowstand (MIS 4 – 3). Finally, OSU6, made of finer-grained flake-shaped limestone clasts, suggests the onset of cooler conditions along the slopes and the action of freeze-thaw on bedrock.

Final Highlights

Grotta Romanelli is one of the few localities in this area of the Mediterranean where 3 RSL markers and PSL indicators are stacked along the same cliff at decreasing elevation from 18 m down to 5,5 m a.s.l.

(MIS 11, MIS 9, MISs 5e). This suggests that this part of the Apulian region, although under an overall long-term tectonic stability, underwent some vertical uplift in the last 350 ka. Further chronological constraints for the uppermost and lowermost RSLs would bring new data for the assessment of a more reliable vertical displacement rate of the Apulian coast. The newly assessed chronology of the sedimentary succession filling the cave indicates an early frequentation of the cave under conditions of relative environmental stability, dominated by debris accumulation at very low sedimentation rates (ca. 1 m in 150 ka). The oldest human and faunal frequentation occurred between MIS 9 and MIS 7, earlier than previously supposed (20). The environmental conditions suddenly changed after the Last Interglacial when soil erosion processes on the surrounding slopes brought fine-grained sediments in the cave. A long-lasting hiatus in the sedimentation is marked by the occurrence of several flowstones and speleothems resting on top of ISU3 and ISU 4 spanning from 112 to 43 ka. The complete and final filling of the cave occurred mostly during the MIS 2 – 1 transition, recording human and animal frequentation once again. Due to the intense excavation activities of the past and the consequent lack of sediment, we assume that different sedimentary environments and conditions may have characterised the cave sector closer to the entrance, probably providing more suitable conditions for human settling, as indicated by the evidence of fire, food and frequentation previously reported. In fact, in the inner part of the cave the elements of anthropogenic origin are anyhow present (see also, 35) although at a minor extent and as minor components, as evidenced also by micromorphological observations. The new chronostratigraphic assessment of Grotta Romanelli infilling deposit allows to redefine several important bioevents for European mammal palaeocommunities and add important information for human presence in the Mediterranean area:

- the occurrence of Stephanorhinus hundsheimensis (Toula, 1902) in ISU1 and ISU2 (29) represents the last occurrence of this taxon in Europe, previously attested at about 600 ka (Isernia Faunal Unit). This effectively suggests that a large revision of the Middle Pleistocene rhinoceros is needed to clarify the evolution of S. hundsheimensis;

- the fireplaces reported by Blanc (20, 21) on top of ISU1 should be referred to Middle Pleistocene hominins (H. neanderthalensis or Homo heidelbergensis Schoetensack, 1908) representing some of oldest fireplaces in Europe Mediterranean area (52, 53);

- referring ISU3 to the Last Interglacial (MISs 5e) or to the oldest substages of MIS 5 implies that the mandible of the historical collection of Blanc ascribed to the Eurasian River otter, Lutra lutra (Linnaeus, 1758) (20, 21, 34) is the oldest record of this species in Europe;

- fossils of Palaeoloxodon antiquus (Falconer & Cautley, 1847) and Hippopotamus amphibius Linnaeus, 1758 from ISU3 were considered among the last occurrences of these taxa in Europe, allowing to hypothesise their survival up to MIS 4 – 3 (22). The new chronology of ISU3 suggests that the straight-tusked elephant and the hippopotamus went extinct after MIS 5 (54);

- the lithic industry of the Middle Pleistocene on top of ISU1 (layer K sensu 20, 21, n = 2) and ISU2 (layer I sensu 20; 21, n = 6), and those from the oldest Late Pleistocene ISU3 (layer G sensu 20; 21; n = more than

1100 artefacts) are attributed to the Mousterian (30, 55). Following the new chronology for Grotta Romanelli, these are the oldest evidence of human technology in the Salentine Peninsula (56).

Methods

Litostratigraphy and facies/microfacies analysis

Lithostratigraphy was investigated by preparing, cleaning, measuring and describing the sections inside the cave and surveying, cleaning, measuring and describing the natural outcrops around and on the cliff just above and below the cave entrance, including those still directly damming the cave entrance. Facies analysis was made at the macroscale in order to get information about the depositional context, the related palaeoenvironment in the surroundings of the cave and the correlation among the different units.

Sedimentary facies in caves are generally based on field description of grain-size, fabric and compositional characteristics of coarse-grained deposits derived by physical and chemical weathering of the bedrock and/or transported by running waters both of karstic and external arrival (56).

However, when cave sediments are fine-grained or very fine-grained, or with weakly developed sedimentary structures or apparent massive structures, the facies analysis can be improved by their study at a scale smaller finer than the field observation, that is micromorphology of undisturbed samples (57, 58). Moreover, in human settled cave environments the investigation at the micro-scale can be useful for the recognition of evidence such as trampling, maddening, fire-use etc. or depositional and post-depositional processes that can be assessed at the micro scale including palaeo-environmental information of paramount importance for the determination of the sedimentary context of artefacts and other human and animal remains (56, 60).

Undisturbed samples were removed by simple extraction with standard Kubiena boxes (10x7 cm) in the field and then prepared at “Servizi per la Geologia” lab (Piombino, Italy) by impregnation with a mixture of resin, styrene, and hardener; curing; cutting into cm-thick slabs; and final preparation of 25-µm thin sections, measuring 95×55 mm (Suppl. Mat 2). Thin sections were analysed under a polarising microscope at the University of Torino at magnifications between x20 and x1,000, using plane-polarised and cross-polarised light. Images were captured by a digital camera for polarising microscopy. Thin-were described following the guidelines proposed by Stoops (61) and after Nicosia and Stoops (62).

Geochronology

Six flowstone and one stalagmite samples were dated with U–Th techniques at the High–Precision Mass Spectrometry and Environmental Change Laboratory (HISPEC), Department of Geosciences, National Taiwan University (63,64). For each sample, clean chipped subsample, 0.5-1 g, were selected, gently crushed, ultrasonicated, and then dried at 50 °C in a class 10,000 clean room (65). The cleanest fragments, 0.05-0.10 g, were picked for U–Th chemistry (63) and instrumental analysis to determine U–Th isotopic and concentration data on a multi–collector inductively coupled plasma mass

spectrometer (MC–ICP–MS), Thermo Electron Neptune (64). Uncertainties in the U–Th isotopic data were calculated offline (66). Half–lives of U–Th nuclides used for age calculation, relative to 1950 AD, are given in Cheng et al. (67). Isotopic and age errors given are two standard deviations of the mean and two standard deviations, respectively, unless otherwise noted.

Morphostratigraphy and geomorphological mapping

Geomorphological and morphostratigraphical investigation were carried on by the classic methods of the field survey in the area surrounding the cave and, on the cliff, above and below the cave entrance. During fieldwork a geomorphological map was sketched by recognising and classifying landforms and related deposits according to their origin (morphogenesis), state of activity and, at the same time with lithostratigraphical survey, describing the sedimentary characteristics and facies of the deposits. The morpho-stratigraphical position of each Stratigraphic Unit was assessed based on its lithostratigraphical and elevation position above the sea level. Similar approach for slope deposits and RSL markers such as marine notches, thus helping to assess different cycles of marine high-stands followed by low-stands. Line drawing sections seaward Grotta Romanelli were realised to underline the chronostratigraphic relationship. The elevation of RSL markers (marine notches and marine terrace below the cave entrance) was measured with total station whereas the elevation of the marine deposits above the cave entrance was measured with GPS and Topo Map.

Declarations

Data Availability Statement

All data generated or analysed during this study are included in this published article (and its supplementary information files).

Acknowledgements

The authors are deeply indebted to the Soprintendenza Archeologia, Belle Arti e Paesaggio delle province di Brindisi e Lecce for the permission of the research and field activities (2015–2017 and 2018–2020, with extension for 2021 due to sanitary emergency by SARS-CoV-2, resp. R. Sardella) (Maria Piccarreta, Laura Masiello and Serena Strafella).

We thank the Castro municipality, Capitanerie di Porto di Castro e di Otranto, Parco Naturale Regionale Costa Otranto S.M. di Leuca-Bosco di Tricase, Ninì Ciccarese and Toto De Santis, Michele Rizzo and the Red Coral team, Don Piero Frisullo and Genesareth for their logistical support. We also wish to thank all members of the Romanelli team and many students for helping during 2015-2021 fieldwork activities. Moreover, we indebted to Luca Lanci (University of Urbino, Italy) and Evdokia Tema (University of Torino, Italy) for their useful comments to the early versions of the manuscript.

This work was funded by Sapienza, University of Rome, with Finanziamento Ricerche di Ateneo 2015, Grandi Scavi 2016 (Grant no: SA116154CD9592F3); Grandi Scavi 2017 (Grant no: SA11715C81468801);

Grandi Scavi 2018 (Grant no: SA1181642D3B3C58); Grandi Scavi 2019 (Grant no: SA11916B513E7C4B); Grandi Scavi 2020 (Grant no: SA120172B2C05E68); Grandi Scavi 2021 (Grant no:SA12117A87BC3F0A).

U-Th dating at the HISPEC was supported by grants from the Science Vanguard Research Program of the Ministry of Science and Technology (110-2123-M-002-009), the National Taiwan University (110L8907 to C.-C.S.), and the Higher Education Sprout Project of the Ministry of Education (110L901001 and 110L8907).

Author contributions

P.P, L.F. and I.M. devised the study, the main conceptual ideas and proof outline. They also carried out the litostratigraphical and morphostratigraphical study. L.F and P.P. worked out all figures. T.Y. and C.C.S. performed the U-Th analysis. P.P. performed the facies/micro facies analysis. F.B. and I.M. provided the micropaleontological data, B.Me. and A.I. provided the other palaeontological data. G.L. and B.Mu. performed the site mapping and provided the archeological data. P.P., L.F., B.Me., A.I., F.B., G.L., B.Mu., R.S. carried out excavations and surveys. R.S., B.Me., F.B., G.L., B.Mu., A.I. contributed to the implementation of the research, to the analysis of the results and worked on the manuscript.

Competing interests

The authors declare no competing interests.

References

1. Peresani, M., Cristiani, E. & Romandini, M. *The Uluzzian technology of Grotta di Fumane and its implication for reconstructing cultural dynamics in the Middle–Upper Palaeolithic transition of Western Eurasia*. J. Hum. Evol. **91**, 36–56. https://doi.org/10.1016/j.jhevol.2015.10.012 *(*2016*).*
2. Moroni, A. et al. *Late Neandertals in central Italy. High-resolution chronicles from Grotta dei Santi (Monte Argentario - Tuscany)*. Quat. Sci. Rev. **217**, 130–151. https://doi.org/10.1016/j.quascirev.2018.11.021 *(*2018*)*
3. Holt, B. et al. *The middle-upper palaeolithic transition in northwest Italy: new evidence from riparo Bombrini (Balzi Rossi, Liguria, Italy)*. Quat. Int. **508**, 148–152. https://doi.org/10.1016/j.quaint.2018.11.032 *(*2018*).*
4. Spinapolice, E. E., et al. *Back to Uluzzo – Archaeological, palaeoenvironmental, and chronological context of the Mid-Upper Palaeolithic sequence at Uluzzo C rock shelter (Apulia, Southern Italy)*. J. Quat. Sci. **37**(*2*), 217–234. https://doi.org/10.1002/jqs.3349 *(*2021*).*
5. Marra, F., Rolfo, M. F., Gaeta, M. & Florindo, F. *Anomalous Last Interglacial Tyrrhenian sea levels and Neanderthal settling at Guattari and Moscerini caves (central Italy)*. Sci. Rep. **10**(*1*), 1–16. https://doi.org/10.1038/s41598-020-68604-z *(*2020*).*
6. Lewin, J. & Woodward, J. C. *Karst Geomorphology and Environmental Change. in*, The Physical Geography of the Mediterranean *(ed.Woodward, J.C.)* 287–317 (*Oxford University Press, Oxford,*

2009).

7. Bar-Matthews, M., Ayalon, A., Kaufman, A. & Wasserburg, G. J. *The Eastern Mediterranean palaeoclimate as a reflection of regional events: Soreq cave, Israel*. Earth and Planet. Sci. Lett. **166** (*1–2*), 85–95. https://doi.org/10.1016/S0012-821X(98)00275-1 *(*1999*).*
8. Woodward, J. C. & Goldberg, P. *The sedimentary records in Mediterranean rockshelters and caves: Archives of environmental change*. Geoarchaeology, **16** (*4*), 327–354 *(*2001*).*
9. Mastronuzzi, G., Quinif, Y., Sansò, P. & Selleri, G. *Middle-Late Pleistocene polycyclic evolution of a stable coastal area 1620 (southern Apulia, Italy)*. Geomorphology, **86**(*3–4*), 393–408. https://doi.org/10.1016/j.geomorph.2006.09.014 *(*2007*).*
10. Benjamin J. et al. *Late Quaternary sea-level changes and early human societies in the central and eastern Mediterranean Basin: an interdisciplinary review*. Quat. Int. **449**, 29–57. https://doi.org/10.1016/j.quaint.2017.06.025 *(*2017*).*
11. Antonioli, F. et al. *Morphometry and elevation of the last interglacial tidal notches in tectonically stable coasts of the Mediterranean Sea*. Earth-Sci. Rev. **185**, 600–623. https://doi.org/10.1016/j.earscirev.2018.06.017 *(*2018*).*
12. Vacchi, M. et al. *Millennial variability of rates of sea-level rise in the ancient harbour of Naples (Italy, western Mediterranean Sea)*. Quat. Res. **93**, 284–298. https://doi.org/10.1017/qua.2019.60 *(*2020*).*
13. Bini, M. et al. *An end to the Last Interglacial highstand before 120 ka: Relative sea-level evidence from Infreschi Cave (Southern Italy)*. Quat. Sci. Rev. **250**, 106658. https://doi.org/10.1016/j.quascirev.2020.106658 *(*2020*).*
14. Lari, M. et al. *The Neanderthal in the karst: first dating, morphometric, and paleogenetic data on the fossil skeleton from Altamura (Italy)*. J. Hum. Evol. **82**, 88–94. https://doi.org/10.1016/j.jhevol.2015.02.007 *(*2015*).*
15. Benazzi, S. et al. *Early dispersal of modern humans in Europe and implications for Neanderthal behaviour*. Nature **479**(*7374*), 525–528. https://doi.org/10.1038/nature10617 *(*2011*).*
16. Columbu, A. et al. *Speleothem record attests to stable environmental conditions during Neanderthal–modern human turnover in southern Italy*. Nat. Ecol. Evol. **4**(*9*), 1188–1195. https://doi.org/10.1038/s41559-020-1243-1 *(*2020*).*
17. Sardella, R. et al. *Grotta Romanelli (Lecce, Southern Italy) between past and future: new studies and perspectives for an archaeo-geosite symbol of the Palaeolithic* in Europe. Geoheritage **11**(*4*), 1413–1432. https://doi.org/10.1007/s12371-019-00376-z *(*2019*).*
18. Forti, L., Mazzini, I., Mecozzi, B., Sigari, D. & Sardella, R. *Grotta Romanelli (Castro, Lecce): un sito chiave del Quaternario mediterraneo*. Geologicamente **2**, 18–27 *(*2020*).*
19. Cosentino, D. & Gliozzi, E. *Considerazioni sulle velocità di sollevamento di depositi eutirreniani dell'Italia meridionale e della Sicilia*. Mem. Soc. Geol. It. **41**, 653–665 *(*1988*).*
20. Blanc, G. A. Grotta Romanelli I. *Stratigrafia dei depositi e natura e origine di essi*. Arch. Antropol. Etnol. **50**, 1–39 *(*1920*).*

21. Blanc, G.A. Grotta Romanelli II. *Dati ecologici e paletnologici*. Arch. Antropol. Etnol. **58**, 1–49 *(*1928*).*
22. Fornaca-Rinaldi, G. & Radmilli, A. M. *Datazione con il metodo 230Th/238U di stalagmiti contenute in depositi musteriani*. Atti Soc. Toscana Sci. Nat. **75** (*1*), 639–646 *(*1968*).*
23. Alessio, M., Bella, F., Bachecchi, F. & Cortesi, C. *University of Rome Carbon-14 dates III*. Radiocarbon **7**, 213–222 *(*1965*).*
24. Vogel, J. C. & Waterbolk, H.T. *Groningen radiocarbon dates IV*. Radiocarbon **5**, 63–202 *(*1963*).*
25. Blanc, G. A. *Sulla presenza di* Alca impennis *Linn. nella formazione superiore di Grotta Romanelli in Terra d'Otranto*. Arch. Antropol. Etnol. **58**, 155–186 *(*1927*).*
26. *Di* Stefano, G., Petronio, C., Sardella, R., Savelloni, V. & Squazzini, E. *Nuove segnalazioni di brecce ossifere nella costa fra Castro Marina e Otranto (Lecce)*. Il Quaternario **5**(*1*), 3–10 *(*1992*).*
27. Bologna, P. et al. *Late Pleistocene mammals from the Melpignano (LE) "Ventarole": preliminary analysis and correlations*. Boll. Soc. Paleont. It. **33**(*2*), 265–274 *(*1994*).*
28. Sardella, R., Bertè, F.D., Iurino, D.A., Cherin, M. & Tagliacozzo, A. *The wolf from Grotta Romanelli (Apulia, Italy) and its implications in the evolutionary history of* Canis lupus *in the Late Pleistocene of Southern Italy*. Quat. Int. **328**, 179–195. https://doi.org/10.1016/j.quaint.2013.11.016 *(*2014*).*
29. Pandolfi, L. et al. *Rhinocerotidae (Mammalia, Perissodactyla) from the middle Pleistocene levels of Grotta Romanelli (Lecce, southern Italy)*. Geobios **51**(*5*), 453–468. https://doi.org/10.1016/j.geobios.2018.08.008 *(*2018*).*
30. Spinapolice, E. *Technologie lithique et circulation des matières premières au Paléolithique moyen dans le Salento (Pouilles, Italie méridionale): perspectives comportementales. Doctoral dissertation, Sapienza Università di Roma and Université de Bordeaux 1, Rome/Bordeaux (*2008*).*
31. Calcagnile, L. et al. *New radiocarbon dating results from the Upper Paleolithic-Mesolithic levels in Grotta Romanelli (Apulia, Southern Italy). Radiocarbon, Selected Papers from the 23rd International Radiocarbon Conference, Trondheim, Norway, 17– 22 June*, 2018. https://doi.org/10.1017/RDC.2019.8 *(2019).*
32. Iannucci, A., Sardella, R., Strani F. & Mecozzi, B. *Size shifts in late Middle Pleistocene to Early Holocene* Sus scrofa *(Suidae, Mammalia) from Apulia (southern Italy): ecomorphological* adaptations? Hystrix **31**(*1*), 10–20. https://doi.org/10.4404/hystrix-00258-2019 *(*2020*).*
33. Mecozzi, B. Meles meles *from Middle Pleistocene to Early Holocene of the Italian Peninsula within the evolutionary of European badgers in the Quaternary*. Paleontogr. Abt. A. *DOI*:10.1127/pala/2021/0100 *(*2021*).*
34. Mecozzi, B. et al. *Rediscovering* Lutra lutra *from Grotta Romanelli (southern Italy) in the framework of the puzzling evolutionary history of Eurasian otters*. PalZ, 1–14. https://doi.org/10.1007/s12542-021-00553-y *(*2021*).*
35. Mecozzi, B. et al. *New human fossil from the latest Pleistocene levels of Grotta Romanelli (Apulia, southern Italy)*. Archaeol. Anthropol. Sci., **14**, 1–4. https://doi.org/10.1007/s12520-021-01491-1 *(*2022*).*

36. Tarquini S., Isola I., Favalli M., & Battistini A. *TINITALY, a digital elevation model of Italy with a 10 meters cell size (Version 1.0) [Data set]*. Istituto Nazionale di Geofisica e Vulcanologia *(INGV)*. https://doi.org/10.13127/TINITALY/1.0 *(*2007*).*
37. Botti, U. *Sulla scoperta di ossa fossili in Terra d'Otranto*. Boll. Regio Com. Geol. **1**, 7–8 *(*1874*).*
38. Tagliacozzo, A. *Archeozoologia dei livelli dell'Epigravettiano finale di Grotta Romanelli (Castro, Lecce) strategie di caccia ed economia di sussistenza in* Grotta Romanelli Nel Centenario Della Sua Scoperta (1900–2000) *(ed Fabri*, *P.*, *E. Ingravallo, E. & Mangia*, *A.*) 169–216 (*Congedo Editore*, *Lecce*, 2003).
39. Pandolfi, L. et al. *Rhinocerotidae (Mammalia, Perissodactyla) from the middle Pleistocene levels of Grotta Romanelli (Lecce, southern Italy)*. Geobios, **51**(*5*), 453–468. https://doi.org/10.1016/j.geobios.2018.08.008 *(*2018*).*
40. Pandolfi, L. et al. *Late Pleistocene last occurrences of the narrow-nosed rhinoceros* Stephanorhinus hemitoechus *(Mammalia, Perissodactyla) in Italy (*2017*).* Riv. It. Paleontol. Strat. **123**(*2*), 177–192.
41. Pirazzoli, P.A. *Marine notches in* Sea-level Research: a manual for the collection and evaluation of data. Norwich*: Geo Books (ed Van de Plassche, O.) 361–400 (Norwich, GeoBooks*, 1986).
42. Trenheil, A. *Coastal notches: Their morphology, formation, and function*. Earth-Sci. Rev. **150**, 285–304. https://doi.org/10.1016/j.earscirev.2015.08.003 *(*2015*).*
43. Trenheil, A. *Modelling coastal notch morphology and developmental history in the Mediterranean*. Geo. Res. J. **9**, 77–90; https://doi.org/10.1016/j.grj.2016.09.003 *(*2016*).*
44. Ferranti, L. et al. *Markers of the last interglacial sea-level high stand along the coast of Italy: tectonic implications*. Quat. Int. **145**, 30–54. https://doi.org/10.1016/j.quaint.2005.07.009 *(*2006*).*
45. Winkler, T. S., *Van* Hengstum, P.J., Horgan, M.C., Donnelly, J.P. & Reibenspies, J.H. *Detrital cave sediments record Late Quaternary hydrologic and climatic variability in northwestern Florida*, USA. Sediment. Geol. **335**<bi>,</bi> 51–65. https://doi.org/10.1016/j.sedgeo.2016.01.022 *(*2016*).*
46. Angelucci, D. E. et al. *A tale of two gorges: Late Quaternary site formation and surface dynamics in the Mula basin (Murcia, Spain)*. Quat. Int. **485**, 4–22. https://doi.org/10.1016/j.quaint.2017.04.006 *(*2017*).*
47. Inglis, R. et al. *Sediment micromorphology and site formation processes during the Middle to Later Stone Ages at the Haua Fteah Cave*, Cyrenaica, Libya. Geoarchaeology **33**(*3*), 328–348. https://doi.org/10.1002/gea.21660 *(*2018*).*
48. Russo Ermolli, E. et al. *The pollen record from Grotta Romanelli (Apulia, Italy): New insight for the Late Pleistocene Mediterranean vegetation and plant use*. Rev. Palaeobot. Palynol. **297**, 104577. https://doi.org/10.1016/j.revpalbo.2021.104577 *(*2022*).*
49. Sigari, D. et al. *New parietal engravings in the Romanelli cave (Apulia, southern Italy). Towards a systematic review*. Antiquity **95** (*384*), 1387–1404<bi>.</bi> https://doi.org/10.15184/aqy.2021.128 *(*2021*).*
50. Cerrone, C., Vacchi, M., Fontana, A. & Rovere, A. *Last Interglacial sea-level proxies in the Western Mediterranean*. Earth Syst. Sci. Data. https://doi.org/10.5194/essd-2021-49 *(*2021*).*

51. Waelbroeck, C. et al. *Sea level and deep water temperature changes derived from benthic foraminifera isotopic records*. Quat. Sci. Rev. **21**(*1–3*), 295–305. https://doi.org/10.1016/S0277-3791(01)00101-9 *(*2002*).*

52. Roebroeks, W. & Villa, P. *On the earliest evidence for habitual use of fire in Europe*. PNAS, **108**(*13*), 5209–5214. https://doi.org/10.1073/pnas.1018116108 *(*2011*).*

53. Sanz, M. et al. *Early evidence of fire in south-western Europe: The Acheulean site of Gruta da Aroeira (Torres Novas*, Portugal). Sci. Rep., **10**(*1*), 1–15. https://doi.org/10.1038/s41598-020-68839-w *(*2020*).*

54. Mecozzi, B. et al. *A reappraisal of the Pleistocene mammals from the karst infilling deposits of the Maglie area (Lecce, Apulia, southern Italy)*. Riv. Ital. Paleontol. Strat. **127**(*2*), 355–382. https://doi.org/10.13130/2039-4942/15776 *(*2021*).*

55. Piperno, M. *L'industria musteriana su calcare di Grotta Romanelli (Otranto).* Mem. Ist. Pal. Um. **2**<bi>, </bi> 69–90 *(*1974*).*

56. Bosch, R. F. & White, W. B. *Lithofacies and transport of clastic sediments in karstic aquifers in* Studies of cave sediments *(ed Sasowsky, I. D. & Mylroie, J.) 1–22 (Springer, Boston, MA.*, 2004).

57. Goldberg, P. & Sherwood S. C. *Deciphering Human Prehistory Through the Geoarcheological Study of Cave Sediments.* Evol. Anthr. Issues, News, and Reviews: Issues, News, and Reviews. **15**(*1*), 20–36; https://doi.org/10.1002/evan.20094 *(*2006*).*

58. Karkanas, P. & Goldberg P. *Micromorphology of Cave Sediments in* Treatise on Geomorphology, *(eds John*, *F.*, *Shroder*, *J. F.* & *Frumkin*, *A.*) 286–297 (*Academic Press*, 2013).

59. Morley, M.W. et al. *Hominin and animal activities in the microstratigraphic record from Denisova cave (Altai Mountains, Russia)*. Sci. Rep. **9**, 13785 https://doi.org/10.1038/s41598-019-49930-3 *(*2019*).*

60. Mallol C. & Goldberg P. *Cave and Rock Shelter Sediments in* Archaeological Soil and Sediment Micromorphology, *(eds Nicosia*, *C.* & *Stoops*, *G.*) 359–381 (*John Wiley and Sons*, 2017).

61. Stoops, G. *Guidelines for Analysis and Description of Soil and Regolith Thin Sections*. *Madison, WI*: *Soil Science Society of America. (*2003*).*

62. Nicosia, C. & Stoops, G. *Archaeological soil and sediment micromorphology*. *John Wiley & Sons (*2017*).*

63. Shen, C. C. et al. *Measurement of attogram quantities of ^{231}Pa in dissolved and particulate fractions of seawater by isotope dilution thermal ionization mass spectroscopy*. Anal. Chem. **75**(*5*), 1075–1079. https://doi.org/10.1021/ac026247r *(*2003*).*

64. Shen, C. C. et al. *High-precision and high-resolution carbonate ^{230}Th dating by MC-ICP-MS with SEM protocols.* Geochim. Cosmochim. Acta **99**, 71–86. https://doi.org/10.1016/j.gca.2012.09.018 *(*2012*).*

65. Shen, C. C. et al. *Variation of initial ^{230}Th/^{232}Th and limits of high precision U–Th dating of shallow-water corals* Geochim. Cosmochim. Acta **72**(*17*), 4201–4223. https://doi.org/10.1016/j.gca.2008.06.011 *(*2008*).*

66. Shen, C. C. et al. *Uranium and thorium isotopic and concentration measurements by magnetic sector inductively coupled plasma mass spectrometry*. Chem. Geol. **185**(*3–4*), 165–17. https://doi.org/10.1016/S0009-2541(01)00404-1 *(*2002*).*

67. Cheng, H. et al. *Improvements in ^{230}Th dating, ^{230}Th and ^{234}U half-life values, and U–Th isotopic measurements by multi-collector inductively coupled plasma mass spectrometry*. Earth Plan. Sci. Let. **371–372**, 82–91. https://doi.org/10.1016/j.epsl.2013.04.006 *(*2013*).*

Figures

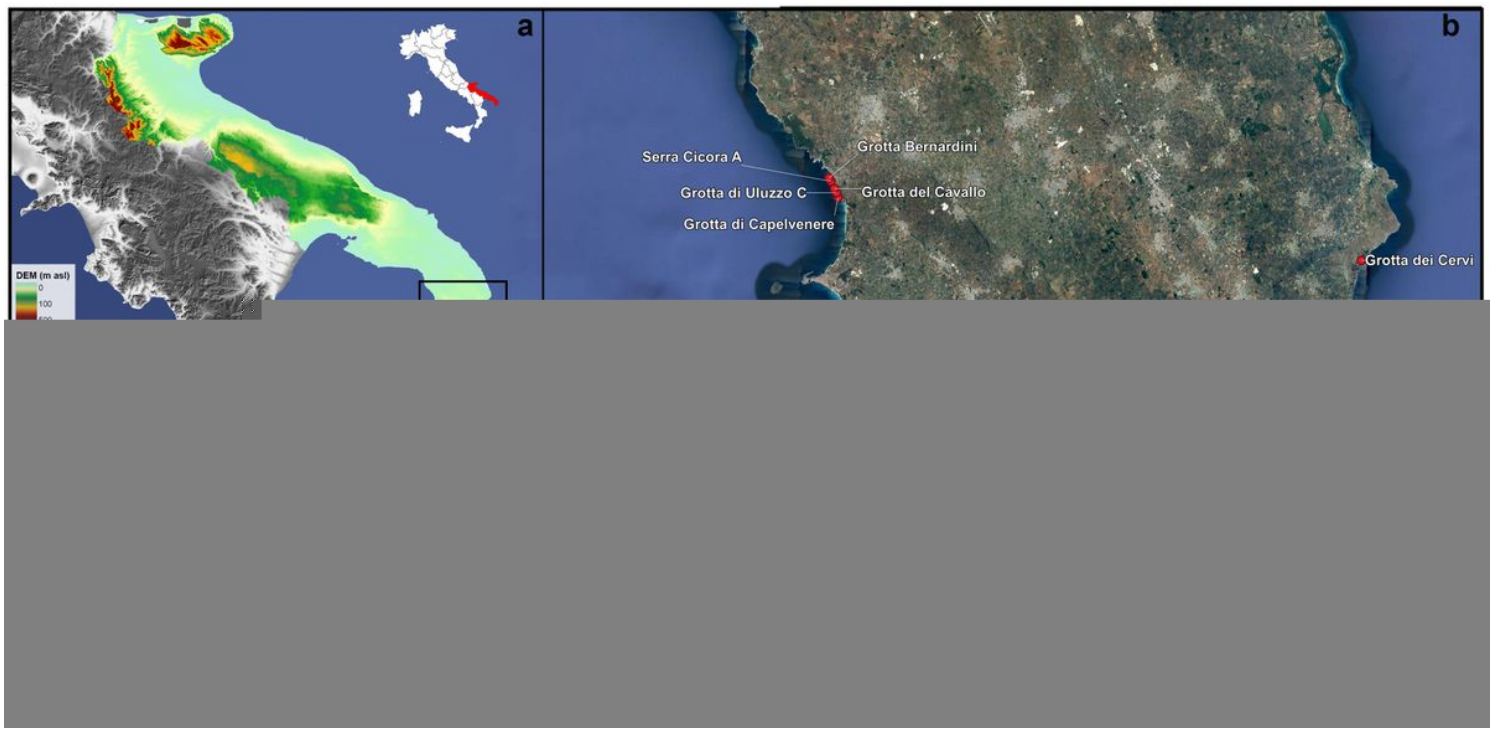

Figure 1

Geographic position of Apulia (map of Italy modified from https://it.wikipedia.org/wiki/File:Italy_map_with_regions.svg) ; Digital Elevation Model of Apulia in southern Italy (elaborated with QGIS 3.16.7 from https://tinitaly.pi.ingv.it/)(36) (a). Satellite image view of the Salentine Peninsula (south-eastern Apulia) (elaborated with QGIS 3.16.7 plugin https://nextgis.com/blog/quickmapservices/) with the known caves filled by Middle to Late Pleistocene deposits (caves position open data from http://www.catasto.fspuglia.it/) (b). The entrance to Grotta Romanelli opening into the limestone cliff (red dot) (c). Elaboration LF.

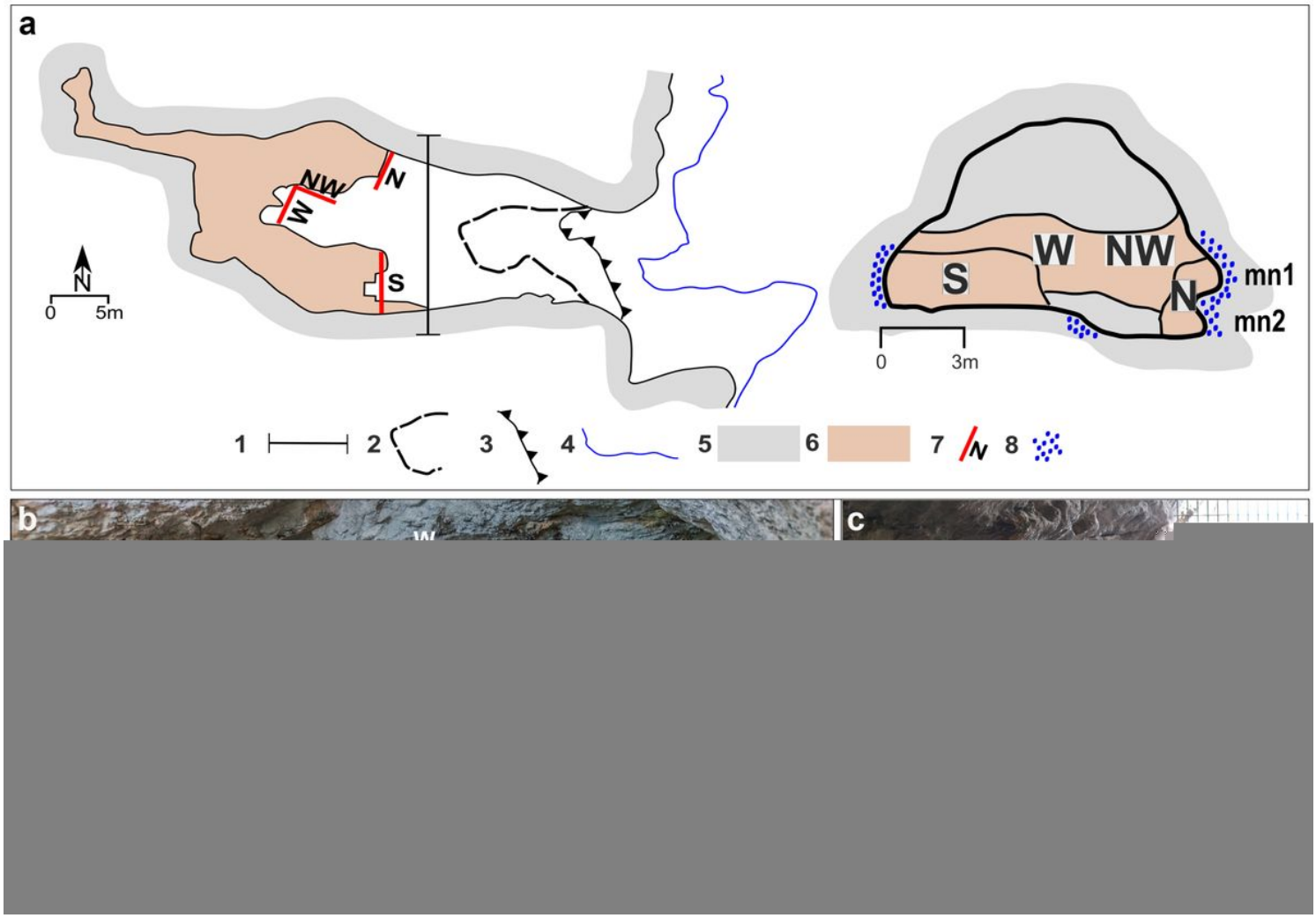

Figure 2

Planimetry of the cave and cave cross section. Legend: 1 Cross section; 2 Cave ceiling limit; 3 Cliff; 4 Sea level; 5 Bedrock; 6 Sedimentary cave filling; 7 Sections location and orientation; 8 Lithophaga burrows (a). Overall view of the cave from the northern side with the location of the described sections (b). The two marine notches (mn1 and mn2) carved into the bedrock and observable on the northern side of the cave, originally buried by the sedimentary succession (c). Artwork and photo PP, LF.

Figure 3

Photos and line drawings of the Sections: Section North (a); Section North-West and West (b); Section South (c). Legend 1 – ISU1; 2 – ISU2; 3 – ISU3; 4 – ISU4; 5 – ISU5; 6 – covered or plan view; 7 – flowstone; 8 - carbonatic crust (acronyms refer to Table 1). Artwork and photo PP, LF

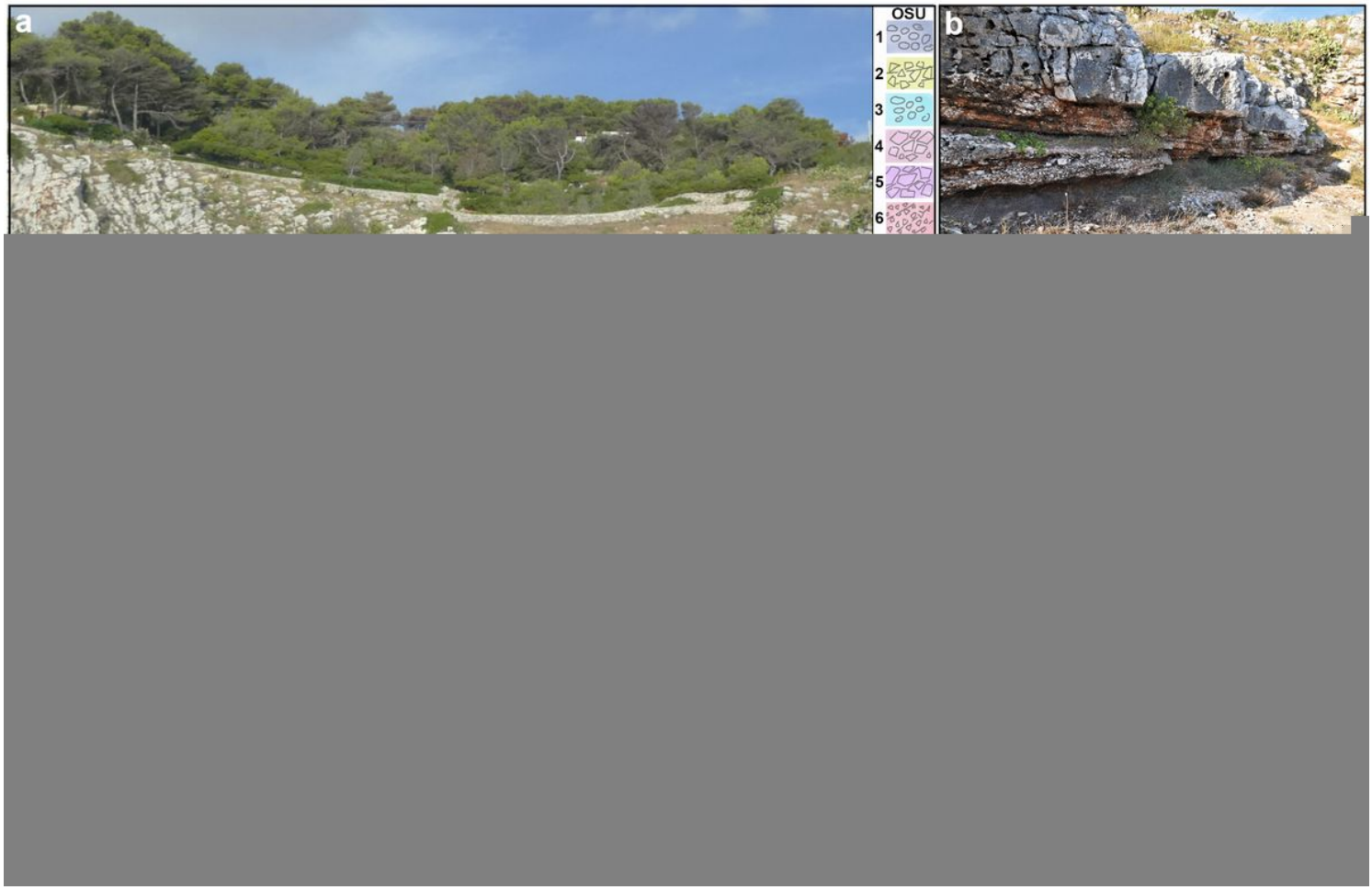

Figure 4

Frontal view of the cave entrance and surrounding cliff and geometry of the O-SU units (a). Detail of marine notches mn1and mn2 (a.1); detail of marine notch mn3 (a.2). Detail of OSU2 (b). Detail of OSU1 (c). Lateral view, towards S, of the marine abrasion platform referred to mn3 (d). View of the different clastic deposits partially covering the entrance of the cave (e). OSU units refer to Table 1. Artwork and photo PP, LF.

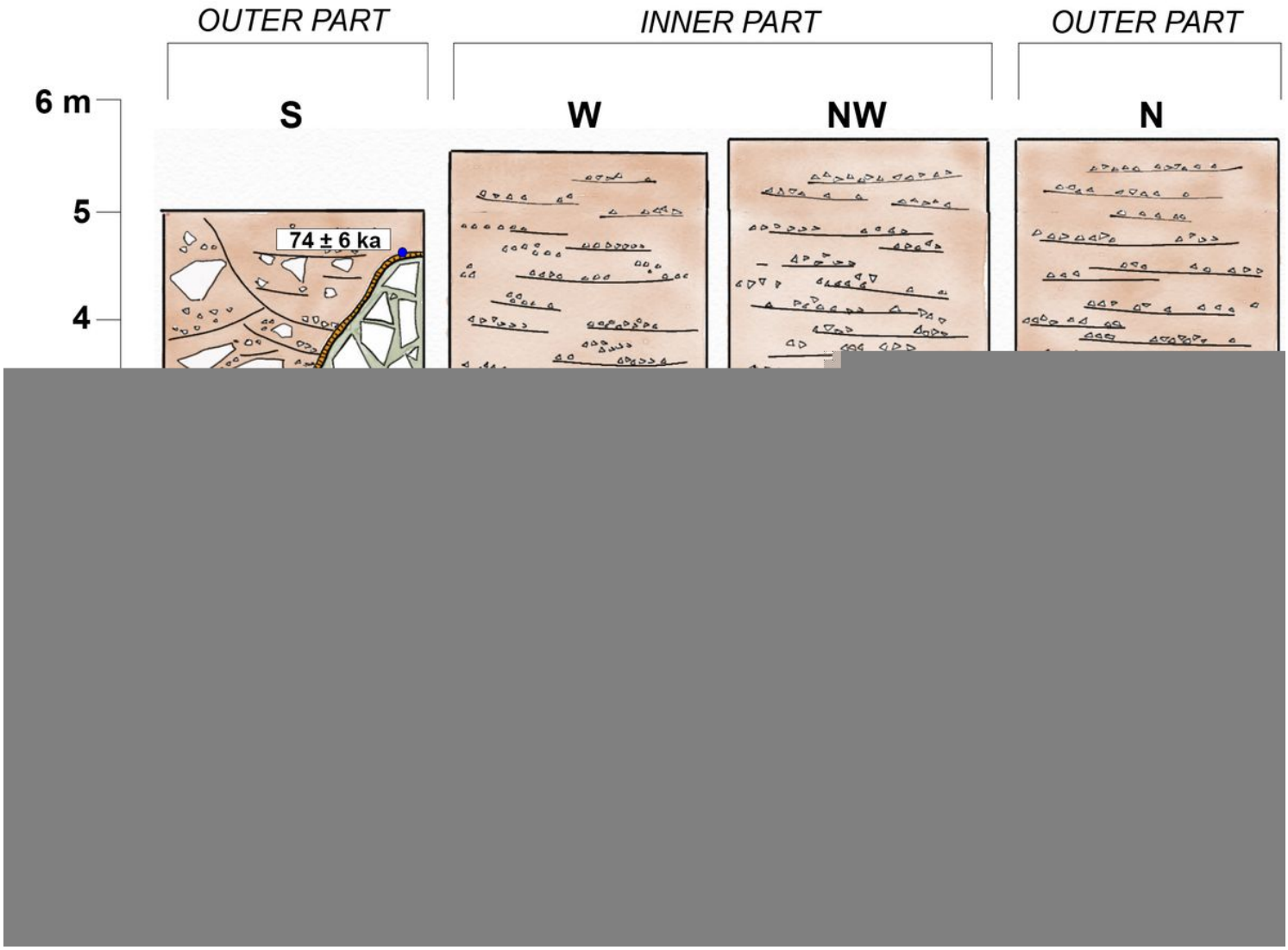

Figure 5

Summary of the succession filling Grotta Romanelli and U/Th dates. Artwork PP.

Figure 6

Correlation between the relative sea level (RSL) markers curve (modified from 51) and the Stratigraphic Units detected inside (ISU) and outside (OSU) the cave. Legend: a- marine notch; b- U/Th dated flowstones; c- fireplace in (21); d- faunal assemblages in (21) and new excavations; e- lithic tools in (21) and new excavations; f- human remains and portable art, new excavations (35,48). Artwork PP, LF.

Figure 7

Evolutionary model for Grotta Romanelli and the surrounding cliff. Referred scale in metres a.s.l. Artwork PP

Supplementary Files

This is a list of supplementary files associated with this preprint. Click to download.

- PieruccinietalSupplementaryMaterial.docx